JOURNAL OF MATERIALS SCIENCE 29 (1994) 436–441

Microstructure characterization of sol–gel derived PZT films

K. HIGUCHI, K. MIYAZAWA, T. SAKUMA
Department of Materials Science, Faculty of Engineering, The University of Tokyo, 7-3-1, Hongo, Bunkyo-ku, Tokyo, Japan
K. SUZUKI
The Institute for Solid State Physics, The University of Tokyo, 7-22-1, Roppongi, Minato-ku, Tokyo, Japan

The crystallization of sol–gel derived amorphous PZT films deposited on a MgO single-crystal substrate and a SiO_2 glass substrate was examined. The pyrochlore crystallites, 5 nm in size, were homogeneously nucleated in the amorphous films at 350 °C. The nucleation temperature of pyrochlore did not depend on the type of substrate. Fine pyrochlore grains were stable even during annealing at high temperatures up to 600 °C. The perovskite formation temperature was dependent on the substrate, and was about 550 °C on the MgO single-crystal substrate and about 750 °C on the SiO_2 glass substrate. The perovskite was heterogeneously nucleated preferentially at the substrate–film interface. Perovskite nucleation was more difficult at the SiO_2 glass–film interface than at the MgO single crystal–film interface. The ease of nucleation reflected the perovskite formation temperature. Perovskite crystals grew fairly rapidly, once they were nucleated in the films. In the multiple-coated films, the interface between successive layers of PZT films was a favourable nucleation site of perovskite, and the columnar perovskite grains passing through the interface were often developed.

1. Introduction

Lead zirconate titanate (PZT) thin films have high potential for electronic and optical devices. There are many techniques by which to prepare PZT films, such as r.f. magnetron sputtering, ion-beam sputtering, laser ablation, sol–gel, MOD (metal organic deposition), MOCVD, etc. Among these techniques, the sol–gel method has been extensively studied in recent years [1–3], because of its manifold advantages in composition control at the molecular level, low-temperature processing, etc.

The crystallization and perovskite formation processes during annealing in sol–gel derived amorphous PZT thin films have been examined by X-ray diffraction (XRD) or electron microscopy (EM) [4–11]. It has been reported that the perovskite is, in general, not formed directly from the amorphous films, but a pyrochlore is generated prior to the perovskite formation. The pyrochlore is formed from temperatures of about 450 °C and remains at high temperatures up to about 600 °C. The generation of pyrochlore is not favourable for the fabrication of PZT thin films with a composition near the morphotropic phase boundary by sol–gel method. Several attempts have been made to lower the perovskite formation temperature, such as rapid heating of amorphous films up to the annealing temperature [9, 12, 13], the deposition of a $PbTiO_3$ interlayer between the substrate and PZT film [10, 14] and high-pressure annealing [10].

In the present work, the crystallization and the perovskite nucleation in amorphous PZT films were examined mainly using electron microscopy to determine the factors deciding the perovskite formation temperature.

2. Experimental procedure

Zirconium tetra-*n*-propoxide, lead acetate trihydrate and titanium tetra-isopropoxide were dissolved in isopropyl alcohol to prepare PZT solution. The ratio of Zr/Ti was kept at 50/50 and the PZT concentration was chosen as 0.4M. Equimolar diethanolamine (DEA) with the alkoxide was added to the solution as a stabilizer [5, 15]. PZT films were obtained from dip-coating by using a substrate of either MgO single crystal or SiO_2 glass. The films were dried at 120 °C for 30 min and fired at 350 °C for 30 min to decompose residual organic matter, and were annealed at temperatures between 350 and 800 °C for 1 h in air. The heating rate was 3 °C min^{-1} up to 350 °C and 1 °C min^{-1} above 350 °C. PZT powders were also obtained from the PZT solution, and were heat treated at temperatures between 350 and 600 °C for 1 h in air.

The films and powders were characterized by scanning electron microscopy (SEM), X-ray diffractometry (XRD), transmission electron microscopy (TEM), and high-resolution transmission electron microscopy

0022-2461

(HRTEM). To prepare TEM samples in cross-section, two coated substrates were pasted face to face, sliced, ground and ion-milled.

3. Results and discussion

3.1. Sol–gel derived PZT powders

XRD profiles of the PZT powders prepared by the sol–gel process are shown as a function of isothermal firing temperature in Fig. 1. PbO crystals are initially formed from amorphous powders at 350 °C, as reported previously [15]. The intensity from the PbO peaks is weakened by annealing at 400 °C. Perovskite formation occurs at temperatures above 450 °C.

The 200 peak separation arising from the tetragonal distortion in perovskite structure was not identified in the powders annealed at temperatures up to 700 °C, therefore the perovskite was regarded as being cubic at room temperature. The tetragonal phase characterized by the peak separation was found in powders annealed at temperatures higher than 750 °C. The tetragonal phase is the equilibrium one at room temperature in PZT with a Zr/Ti atomic ratio of 50/50 [16]. Because the perovskite is cubic at annealing temperatures above 400 °C [16], the cubic to tetragonal (c–t) transformation must be suppressed during cooling, in powders annealed at up to 700 °C, but is induced in powders annealed at higher temperatures. The result may be related to the grain-size effect. The average grain size of PZT powders depends on the annealing temperature. The powders annealed at 700 and 750 °C have a grain size of 0.14 and 0.20 μm, respectively. It has been reported that the c–t transformation is suppressed in fine-grained powders of $BaTiO_3$ and $PbTiO_3$ with grain sizes less than a critical value. The critical grain size is about 0.1 μm for $BaTiO_3$ [17] and 0.02 μm for $PbTiO_3$ [18]. The critical grain size may be between 0.14 and 0.20 μm in the PZT powders.

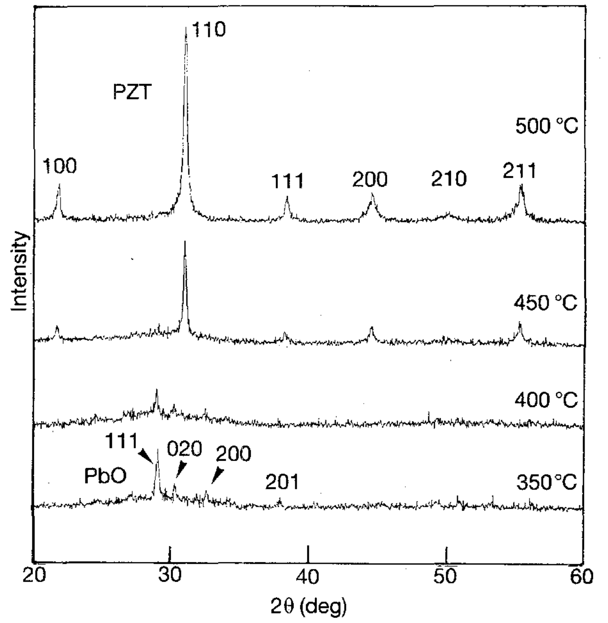

Figure 1 XRD profiles of PZT powders annealed at various temperatures for 1 h.

3.2. Single-coated PZT films

3.2.1. Film thickness control

The film thickness obtained by a single dip-coating process is expressed as [19]

$$t = a(\mu U/\rho g)^{1/2} \qquad (1)$$

where a is a constant, μ the viscosity, U the drawing rate, ρ the density of the liquid, and g the gravitational acceleration, respectively. It is necessary to modify Equation 1 to evaluate the thickness of the annealed films by taking into account the evaporation of solvent, as follows

$$t = a'c(\mu/\rho)^{1/2} \qquad (2)$$

where c is the concentration of PZT solution and a' is a constant, which includes U and g for a constant drawing rate. Note that μ and ρ vary with c, and then t does not change linearly with c. The film thickness is plotted against $c(\mu/\rho)^{1/2}$ in Fig. 2. A linear relationship is obtained between t and $c(\mu/\rho)^{1/2}$ as expected from Equation 2. The result means that the thickness of a single-coated film can be controlled by properly choosing the parameter of $c(\mu/\rho)^{1/2}$.

3.2.2. Effect of substrate on crystallization of PZT films

Figs 3 and 4 show the XRD profiles of annealed PZT films on a MgO single-crystal substrate and a SiO_2 glass substrate. On both substrates, the perovskite is not directly formed from amorphous films but the pyrochlore appears prior to the perovskite. In other words, the crystallization of amorphous PZT films is initiated by the formation of pyrochlore crystals. The crystallization temperature depends on the substrate; on MgO single-crystal substrate, the peaks from pyrochlore are clearly detected at 500 °C and those from perovskite are identified above 550 °C in Fig. 3, while on the SiO_2 glass substrate, the peaks from pyrochlore first clearly appear at 650 °C and those from perov-

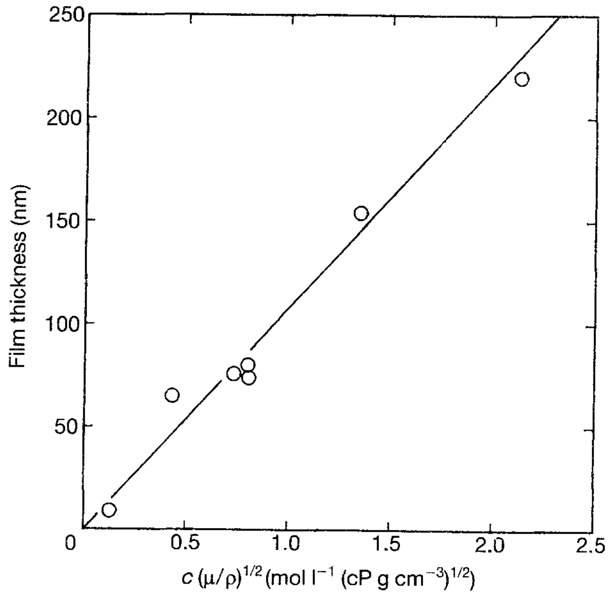

Figure 2 A relationship between the thickness of the PZT film annealed at 600 °C and a parameter $c(\mu/\rho)^{1/2}$.

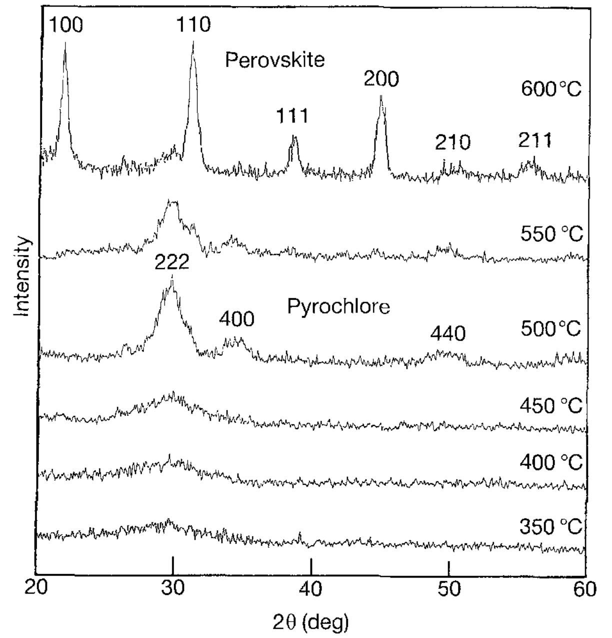

Figure 3 XRD profiles of PZT films annealed at various temperatures for 1 h on a MgO single-crystal substrate.

skite are seen at 750 °C in Fig. 4. It should be noted that the pyrochlore nucleation temperature determined by the XRD analysis is not accurate. Electron microscopy has revealed that very fine pyrochlore crystallites, 5 nm in size, have already been nucleated at the initial firing temperature of 350 °C in films deposited on both MgO single crystal and SiO_2 glass substrates. The generation of such fine pyrochlore crystallites cannot be detected with conventional XRD analysis. The results of the electron microscopy will be discussed later in more detail.

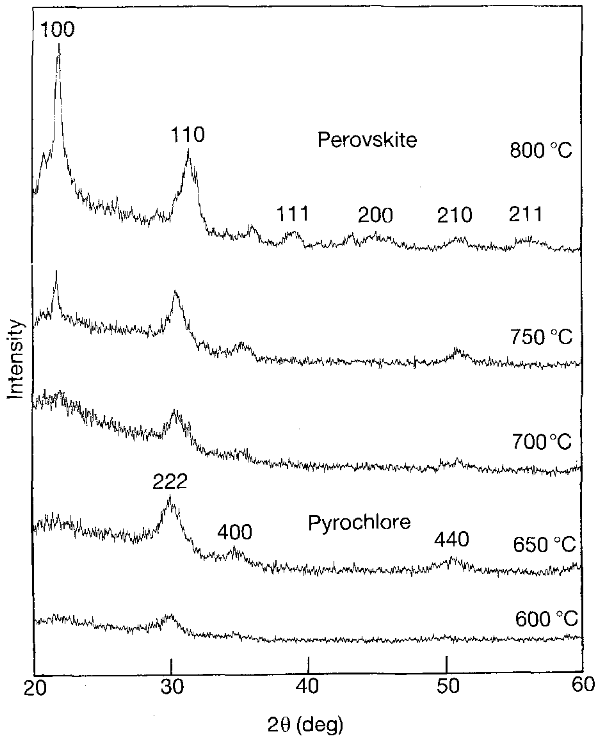

Figure 4 XRD profiles of PZT films annealed at various temperatures for 1 h on a SiO_2 glass substrate.

The perovskite formation temperature is lower by about 200 °C on the MgO single-crystal substrate than on the SiO_2 glass substrate. The MgO single-crystal substrate is favourable for the perovskite formation in PZT films in comparison with the SiO_2 glass substrate. The perovskite formed in the films on both substrates is identified to be cubic at room temperature. In each film, PbO is not found during crystallization in contrast to the PZT powders as described before. The surface of fine powders must be a nucleation site for PbO crystals. On the basis of the results, MgO single-crystal substrate was mainly used in our experiments.

3.2.3. Microstructure of single-coated films

Fig. 5 is a dark-field TEM image of the cross-section of the film annealed at 350 °C. The major spots in the diffraction pattern originate from the MgO single-crystal substrate, and the broad and faint ring emanates from PZT films. In the XRD profiles of Fig. 3, the films are regarded to be fully amorphous at 350 °C. However, the micrograph reveals that fine crystallites have already been generated in the amorphous film after annealing at 350 °C. The fine crystallites are more clearly imaged in the HRTEM image of Fig. 6. The (2 2 2) and (4 0 0) lattice fringe spacings of the crystallites are close to the (2 2 2) or (4 0 0) lattice spacing of pyrochlore with a lattice constant of 1.04 nm, which was determined from the XRD analysis. The pyrochlore crystallites with a grain size of about 5 nm are uniformly distributed in the amorphous matrix. It seems that the pyrochlore crystallites are homogeneously nucleated in the amorphous film.

The pyrochlore formation temperature in amorphous PZT films has been reported to be above 400 °C from the XRD analysis [9, 12, 21]. The present XRD results exhibit a slightly higher pyrochlore formation temperature than that in the previous ones. However,

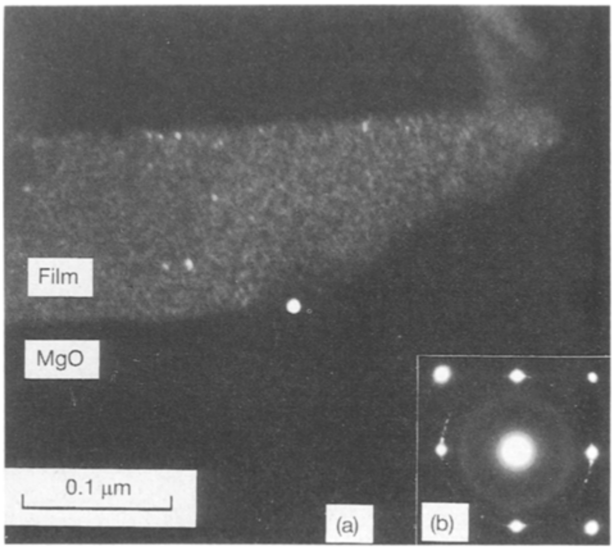

Figure 5 (a) A dark-field TEM image of a cross-section of the single-coated PZT film annealed at 350 °C taken by 2 2 2 reflection of pyrochlore ring pattern. (b) A selected-area diffraction pattern taken along a [0 0 1] zone axis in the MgO single-crystal substrate.

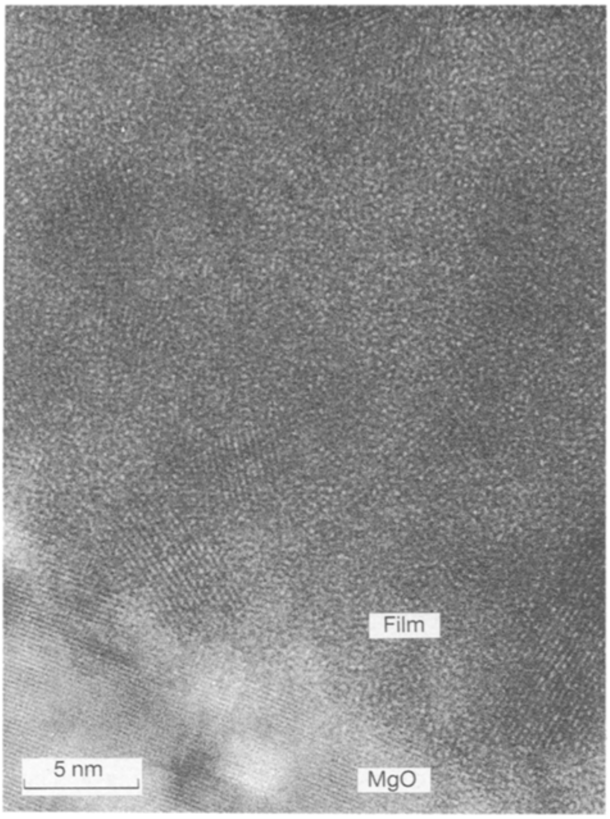

Figure 6 A HRTEM image of the single-coated PZT film annealed at 350 °C. Note that small crystallites are formed at the annealing temperature.

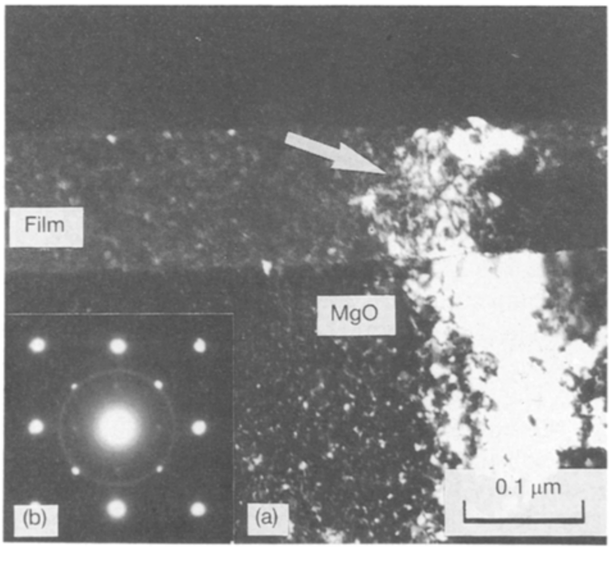

Figure 7 (a) A dark-field TEM image of the cross-section of the single-coated PZT film annealed at 600 °C. The dark-field image was taken with using 2 2 2 reflection of the pyrochlore, 0 1 0 reflection of the perovskite and 0 2 0 reflection of the substrate. (b) A selected-area diffraction pattern whose beam direction is close to the [0 0 1] zone axis in the MgO single-crystal substrate.

the HRTEM observation has revealed that the pyrochlore crystallites are generated at lower temperature of 350 °C in the films coated on both MgO single crystal and SiO_2 glass substrates. Because the pyrochlore is homogeneously nucleated, the nucleation temperature must not be dependent on the substrate.

Fig. 7 shows a cross-section of the film annealed at 600 °C for 1 h. In the diffraction pattern of Fig. 7, spots other than major ones from the MgO single-crystal substrate are indexed for perovskite structure. The perovskite reflections arise from a coarse grain indicated by an arrow in Fig. 7. The grain is dislocated and the grain boundaries are very rugged. The 2 2 2 ring spacing of the fine pyrochlore grains does not precisely coincide with that of 1 1 0 spots from the coarse perovskite grain. The (2 2 2) lattice spacing of the pyrochlore is slightly larger than the (1 1 0) lattice spacing of the perovskite. The result is consistent with the XRD data in Fig. 4. The ring patterns originated from the pyrochlore phase become sharper in Fig. 7 than in Fig. 5. This is caused by the fact that the amorphous phase is almost completely crystallized at 600 °C. The pyrochlore crystals still retain a very fine grain size of about 5 nm. Fine grains of the pyrochlore are extremely stable in the film, while the perovskite grain size is of the order of 0.1 μm. It is noted that the perovskite always appears as coarse grains in the film [7, 8, 22, 23] and that the perovskite formation temperature depends on the substrate [5, 6, 14]. It is possible to speculate that the perovskite is heterogeneously nucleated in the film and grows fairly rapidly, once it nucleates. Judging from the fact that the coarse grain has a particular orientation relationship with the substrate, the substrate–film interface must be a possible nucleation site of the perovskite. The nucleation of perovskite at the MgO single crystal–film interface must be easier than at the SiO_2–film interface, because the perovskite formation temperature is 550 °C on the MgO single-crystal substrate and 750 °C on SiO_2 glass substrate. The perovskite formation temperature decreases with the enhancement of nucleation. Kwok and Desu [10] have reported that the nucleation is enhanced by high-pressure annealing or by the presence of the $PbTiO_3$ interlayer between film and substrate. Tuttle *et al.* [7] have insisted that the perovskite nucleates preferentially and heterogeneously from platinum crystallites of the $Pt/SiO_2/Si$ substrate or from stress hillocks protruding from the bottom electrode. These data support the view that the perovskite formation temperature is determined by nucleation sites.

The diffraction pattern in Fig. 7 shows that the coarse perovskite grain has an epitaxial relationship with the substrate. It may be possible to produce the perovskite films with a particular orientation by suitably choosing the type of substrate and by realizing the epitaxial growth condition.

3.3. Multiple-coated films

Fig. 8 is a dark-field image of a cross-section of the PZT film annealed at 600 °C. The film was prepared by repeating the coating and annealing processes five times. Each coated layer has almost the same thickness of about 0.1 μm. The total thickness of multiple-coated films can be controlled by regulating the thickness of the single layer and the coating times. Columnar grains are observed throughout the film. The width of the columnar grains is about 0.1 μm.

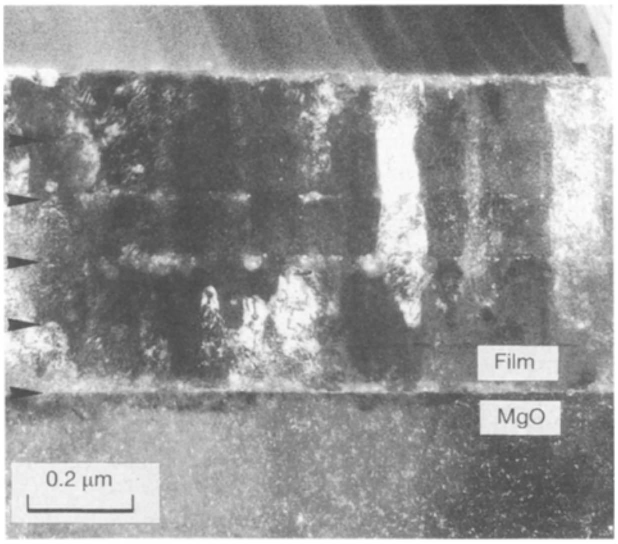

Figure 8 A dark-field TEM image of the cross-section of the multiple-coated PZT film annealed at 600 °C. The arrows indicate the interface of the layers and the interface between the film and substrate.

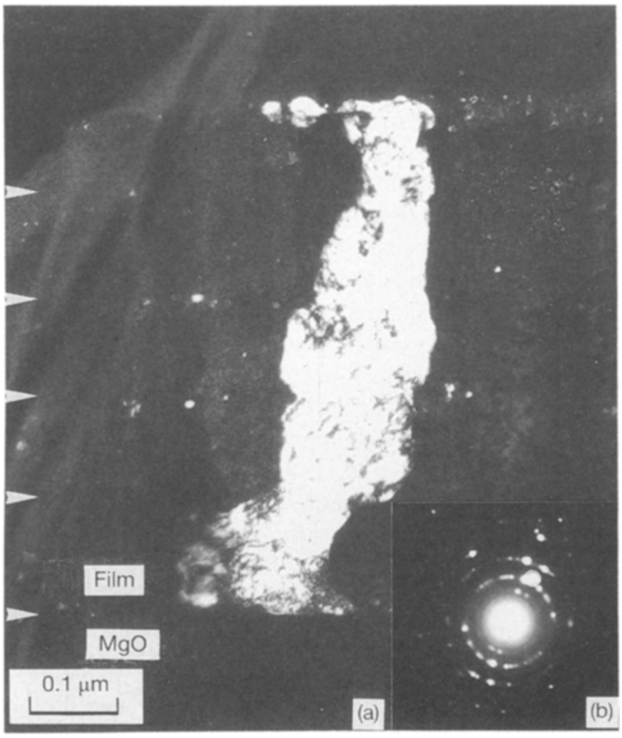

Figure 9 A dark-field TEM image of a columnar grain in the PZT film annealed at 600 °C. The arrows indicate the interface of the layers and the interface between the film and substrate.

Fig. 9 shows one of the columnar grains through a successively coated layer in the film. This grain is confirmed to be a single crystal. The strain-field contrast in the grain may be associated with the internal stress caused by the difference of the thermal expansion coefficient between the film and the substrate. The columnar grain grows through the interface between the layers. It is possible to expect that if the bottom layer is perovskite, the next upper layer easily becomes perovskite with an epitaxial relationship with the lower one.

No preferred orientation of columnar perovskite grains was found in XRD data. The nucleation of columnar grains must occur not only at the substrate–film interface but also at the interface between the layers. In the latter case, the columnar grain will not have an epitaxial orientation relationship with the MgO single-crystal substrate. In fact, some of the columnar grains are not in contact with the substrate, as seen in Fig. 8. It is important that the nucleation of perovskite grains is enhanced with multiple coating, because the interface between the layers becomes a nucleation site as well as the substrate–film interface. Because the perovskite crystal in a lower layer becomes a favourable nucleation site for perovskite in an upper layer, the perovskite substrate may be suitable for fabricating perovskite thin films.

Many fine pyrochlore grains in the first layer remaining after the first annealing, disappeared during successive coating and annealing processes. The growth of perovskite grains from the second layer towards the first layer may take place during the second annealing at the expense of fine pyrochlore grains, in addition to the growth of perovskite in the first layer. However, some pyrochlore grains remained even after the final annealing, as seen in Fig. 8. These fine grains are mostly located at the interface between the substrate and the first layer. The complete disappearance of these fine grains is necessary for synthesis of a single perovskite phase film.

4. Conclusions

The microstructures of sol–gel derived PZT films on a MgO single-crystal substrate and a SiO_2 glass substrate were examined. The following results were obtained.

1. The pyrochlore is initially crystallized in amorphous PZT films at the annealing temperature of 350 °C. Fine pyrochlore grains, about 5 nm in size, are homogeneously formed in the films and their formation temperature does not depend on the type of substrate. The fine grain size of the pyrochlore is very stable.

2. The perovskite formation temperature is 550 °C for MgO single-crystal substrate and 750 °C for SiO_2 glass substrate. The perovskite is heterogeneously nucleated preferentially at the substrate–film interface. The nucleation of perovskite is more difficult at the SiO_2 glass–film interface than MgO single-crystal–film interface. Even at the MgO single-crystal–film interface, the perovskite is not easily nucleated, but grows fairly rapidly after nucleation. The perovskite grains nucleated at the interface often have an epitaxial relationship with the MgO single-crystal substrate.

3. In the multiple-coated films, the interface between successive layers is favourable for perovskite nucleation. The columnar perovskite grains, about 0.1 µm wide, are developed through the layers.

4. The crystallization process of PZT films is different from PZT powders produced by the sol–gel method. The PbO crystals are nucleated in the powders prior to perovskite formation.

Acknowledgement

This work was supported by the Grant-in-Aid for Scientific Research of the Ministry of Education, Science and Culture, Japan (Subject no. 04453059).

References

1. D. R. UHLMANN, G. TEOWEE, J. M. BOULTON, S. MOTAKEF and S. C. LEE, *J. Non-Cryst. Solids* **147 148** (1992) 409.
2. G. YI and M. SAYER, *Am. Ceram. Soc. Bull.* **70** (1991) 1173.
3. Y. XU and J. D. MACKENZIE, *Integr. Ferroelect.* **1** (1992) 17.
4. H. SAKAI and T. TUCHIYA, *J. Ceram. Soc. Jpn* **99** (1991) 630.
5. Y. TAKAHASHI and K. YAMAGUCHI, *J. Mater. Sci.* **25** (1991) 3950.
6. N. TOHGE, S. TAKAHASHI and T. MINAMI, *J. Am. Ceram. Soc.* **74** (1991) 67.
7. B. A. TUTTLE, T. J. HEADLEY, B. C. BUNKER, R. W. SCHWARTZ, T. J. ZENDER, C. L. HERNANDEZ, D. C. GOODNOW, R. J. TISSOT, J. MICHAEL and A. H. CARIM, *J. Mater. Res.* **7** (1992) 1876.
8. K. C. CHEN and J. D. MACKENZIE, *Mater. Res. Soc. Symp. Proc.* **180** (1990) 663.
9. B. A. TUTTLE, R. W. SCHWARTZ, D. H. DOUGHTY and J. A. VOIGT, *ibid.*, **200** (1990) 159.
10. C. K. KWOK and S. B. DESU, *ibid.*, **271** (1992) 371.
11. C. H. PENG, S. W. PARK and S. B. DESU, *Ceram. Trans.* **25** (1992) 169.
12. J. CHEN, K. R. UDAYAKUMAR, K. G. BROOKS and L. E. CROSS, *J. Appl. Phys.* **71** (1992) 4465.
13. S. HIRANO, T. YOGO, K. KIKUTA, K. KATO, W. SAKAMOTO and S. OGASAHARA, *Ceram. Trans.* **25** (1992) 19.
14 S. L. SWARTZ, S. J. BRIGHT and J.R. BUSCH, *ibid.*, **14** (1990) 159.
15. Y. TAKAHASHI, Y. MATSUOKA, K. YAMAGUCHI, M. MATSUKI and K. KOBAYASHI, *J. Mater. Sci.* **25** (1991) 3960.
16. B. JAFFE, W. R. COOK and H. JAFFE, "Piezoelectric Ceramics" (Academic Press, London, 1971).
17. K. UCHINO, E. SADANAGA and T. HIROSE, *J. Am. Ceram. Soc.* **72** (1989) 1555.
18. K. ISHIKAWA, *Phys. Rev. B Condens. Matter* **37** (1988) 5852.
19. L. E. SCRIVEN, *Mater. Res. Soc. Symp. Proc.* **121** (1988) 717.
20. A. H. CARIM, B. A. TUTTLE, D. H. DOUGHTY and S. L. MARTINEZ, *J. Am. Ceram. Soc.* **74** (1991) 1455.
21. C. K. KWOK, S. B. DESU and L. KAMMERDINER, *Mater. Res. Soc. Symp. Proc.* **200** (1990) 83.
22. S. A. MYERS and L. N. CHAPIN, *ibid.*, **200** (1990) 231.
23. C. K. KWOK and S. B. DESU, *Ceram. Trans.* **25** (1992) 85.

Received 5 February
and accepted 14 June 1993